



Published in final edited form as:

Oncogene. 2012 November 22; 31(47): 4898–4911. doi:10.1038/onc.2011.656.

Acquired cancer stem cell phenotypes through Oct4-mediated dedifferentiation

Suresh M. Kumar¹, Shujing Liu¹, Hezhe Lu², Hongtao Zhang¹, Paul J. Zhang¹, Phyllis A. Gimotty³, Matthew Guerra³, Wei Guo², and Xiaowei Xu¹

¹Department of Pathology and Laboratory Medicine, University of Pennsylvania, Philadelphia, PA 19104

²Department of Biology, University of Pennsylvania, Philadelphia, PA 19104

³Department of Biostatistics and Epidemiology, University of Pennsylvania, Philadelphia, PA 19104

Abstract

There is enormous interest to target cancer stem cells (CSCs) for clinical treatment because these cells are highly tumorigenic and resistant to chemotherapy. Oct4 is expressed by CSC-like cells in different types of cancer. However, function of Oct4 in tumor cells is unclear. In this study, we showed that expression of *Oct4* gene or transmembrane delivery of Oct4 protein promoted dedifferentiation of melanoma cells to CSC-like cells. The dedifferentiated melanoma cells showed significantly decreased expression of melanocytic markers and acquired the ability to form tumor spheroids. They showed markedly increased resistance to chemotherapeutic agents and hypoxic injury. In the subcutaneous xenograft and tail vein injection assays, these cells had significantly increased tumorigenic capacity. The dedifferentiated melanoma cells acquired features associated with CSCs such as multipotent differentiation capacity and expression of melanoma CSC markers such as ABCB5 and CD271. Mechanistically, *Oct4* induced dedifferentiation was associated with increased expression of endogenous *Oct4*, *Nanog* and *Klf4*, and global gene expression changes that enriched for transcription factors. RNAi mediated knockdown of *Oct4* in dedifferentiated cells led to diminished CSC phenotypes. Oct4 expression in melanoma was regulated by hypoxia and its expression was detected in a subpopulation of melanoma cells in clinical samples. Our data indicate that Oct4 is a positive regulator of tumor dedifferentiation. The results suggest that CSC phenotype is dynamic and may be acquired through dedifferentiation. Oct4 mediated tumor cell dedifferentiation may play an important role during tumor progression.

Users may view, print, copy, download and text and data- mine the content in such documents, for the purposes of academic research, subject always to the full Conditions of use: http://www.nature.com/authors/editorial_policies/license.html#terms

Correspondence should be addressed to: Xiaowei Xu, MD, PhD, Department of Pathology and Laboratory Medicine, University of Pennsylvania School of Medicine, 3400 Spruce Street, Philadelphia, PA 19104, xug@mail.med.upenn.edu.

Conflict of Interest

The authors declare no conflict of interest.

The authors declare that they have no competing financial interests.

Keywords

Oct4; Cancer stem cell; Melanoma; Dedifferentiation; hypoxia

Introduction

The successful reprogramming of somatic cells to induced pluripotent stem (iPS) cells indicates that differentiated cells retain the capacity to revert to immature cells. *Oct4*, *Sox2*, *c-Myc*, *Klf4*, *Nanog* and *Lin28* have been used for somatic cell reprogramming (Takahashi et al. 2007; Yu et al. 2009). *Oct4* is the most critical transcription factor since it can reprogram adult stem cells to iPS cells as a single factor (Kim et al. 2009). Tumorigenesis and somatic cell reprogramming share common mechanisms (Daley 2008). Aberrant expression of *Oct4*, *Nanog*, *Sox2*, *Lin28* and *Klf4* are all associated with abnormal tissue growth or tumorigenesis (Hochedlinger et al. 2005; Chen et al. 2008; Viswanathan et al. 2009; Schoenhals et al. 2009). Poorly differentiated tumors show preferential overexpression of genes normally enriched in embryonic stem cells (ESCs), such as downstream targets of *Nanog*, *Oct4*, *Sox2* and *c-Myc* (Ben-Porath et al. 2008). p53 is a critical negative regulator of somatic cell reprogramming, and virtually all cancer cells lose p53 function in one way or another (Kawamura et al. 2009; Hanna et al. 2009). These data suggest that the reprogramming factors may be involved in tumor progression.

Tumor dedifferentiation is a well known phenomenon and it has long been proposed to be involved in tumor progression (Gabbert et al. 1985). Similar to somatic cell reprogramming, tumor dedifferentiation is reversal of cell development to a more immature state. Dedifferentiated melanoma cells is known to lose pigmentation (Bennett 1983). Cancer stem cells (CSCs) have dedifferentiated phenotypes and it has been shown that CD271+ melanoma CSCs lack expression of common melanocytic markers (Boiko et al. 2010). However, the mechanism underlying tumor dedifferentiation is not fully understood.

There is enormous interest to find the origin of CSCs and target these cells for therapy. Oct4 has been proposed as a biomarker for CSC-like cells. Oct4 is detectable in a variety of cancer types including melanoma (Strizzi et al. 2008) and CSC-like cells are enriched for Oct4 expression (Zhang et al. 2010; Hu et al. 2010; Liu et al. 2010; Peng et al. 2010; Saigusa et al. 2009). It has been shown that Oct4 expression is associated with differentiation state of cancer cells (Zhang et al. 2010; Chen et al. 2009). Oct4 expression increases in the residual breast cancer cells after treatment (Magnifico et al. 2009) and its expression is associated with worse clinical outcome (Saigusa et al. 2009; Zhang et al. 2010). Knockdown of *Oct4* results in breast CSC-like cell apoptosis (Hu et al. 2008). Nevertheless, function of Oct4 in cancer cells is still unclear and it is unknown whether Oct4 has similar function in normal cells and cancer cells.

In this report, we showed for the first time that forced expression of *Oct4* gene or transmembrane delivery of Oct4 protein induces dedifferentiation of melanoma cells, and the dedifferentiated melanoma cells acquire CSC phenotypes. Mechanistically, Oct4 induces re-activation of reprogramming factors in melanoma cells and global gene expression changes that enriched for transcription factors. The acquisition of CSC phenotypes induced

by Oct4 is distinctively different from epithelial-mesenchymal transition (EMT) induced changes. In addition, we showed that Oct4 expression in melanoma is regulated by hypoxia.

Results

Oct4 induces dramatic morphological changes in tumor cells

We infected six different melanoma cell lines (WM35, WM793, WM9, WM115A, WM3523A and 1205Lu) with lentiviruses expressing *Oct4*. After infection, morphological changes were quickly apparent with well-formed colonies emerging 5-7 days after infection (Fig. 1a). These Oct4 expressing melanoma colonies had morphological features analogous to those transformed colonies seen during iPS cell induction. When Oct4 expressing melanoma cells were seeded onto mouse embryonic fibroblasts (MEFs) and cultured in human embryonic stem cells culture medium (hESCM4), they retained the raised colony morphology and did not display typical morphology of hESC-like colonies (Supplementary Information, Fig. S1a). The colonies were negative for alkaline phosphatase, a marker for pluripotent stem cells (data not shown). Melanoma cells infected with green fluorescent protein (GFP)-containing lentiviruses did not display any morphological changes (Fig. 1a). When the colony-forming Oct4 expressing melanoma cells were transferred to hESCM4 without MEFs, five of the six melanoma cell lines formed floating spheres with morphologies similar to embryoid bodies (Fig. 1a and Supplementary Information Fig. S1b), whereas the GFP infected melanoma cells did not survive in this same medium (Fig. 1a). While Oct4-infected 1205Lu cells did not form spheres in hESCM4, they proliferated well in this medium. To ensure that the effect seen was due to *Oct4* and not related to the viral vector used, we infected WM35 cells with a different lentiviral Oct4 vector tagged with GFP. Oct4-GFP infected WM35 cells cultured in the hESCM4 media formed spheres similar to Oct4-WM35 cells (Supplementary Information Fig. S1c). To further confirm that the sphere forming cells were not due to contamination by other stem cells used in the laboratory, we performed DNA fingerprinting studies. The results of these studies showed that the Oct4-sphere-forming cells were the same cells as their parental cells (Supplementary Information Table 1).

Oct4 induces dedifferentiation of melanoma cells

Next we examined expression levels of Oct4 in sphere-forming cells by Western blotting. We found that these sphere forming cells expressed Oct4 at levels similar to those seen in human Tera-2 embryonic carcinoma (hEC) cells, whereas the parental tumor cells expressed little Oct4 (Fig. 1a). Genotyping PCR confirmed that the colony-forming cells carried the *Oct4* transgene (Supplementary Information Fig. S2).

Histological and immunohistochemical analyses showed that the Oct4 induced melanoma spheres were composed of immature cells with high nucleus/cytoplasm ratios (see Supplementary Information Fig. S3a). We found that melanocytic markers were significantly down-regulated in these cells. Only few tumor cells in these spheres expressed S-100 protein (*S100A* and *S100B*) and tyrosinase (*TYR*) (see Supplementary Information Fig. S3a). In contrast, tumor cells in the spheres uniformly expressed Oct4 in the nuclei (Fig. 1b). To test whether the effect of Oct4 was cell type dependent, we infected foreskin derived

normal melanocytes with the same Oct4-lentiviruses. Oct4-melanocytes retained their bipolar morphology and spheroids were not detected after 14-28 days of infection (data not shown). These results indicated that normal melanocytes cannot be dedifferentiated by *Oct4* alone.

Oct4 induces more aggressive biological behavior

We next examined whether the dramatic morphological changes following *Oct4* infection were accompanied by significant changes in proliferation, colony formation, and survival. Same amount of cells were seeded initially and cell proliferation was measured 24, 48 and 72 hours later. Oct4 infected cells proliferated significantly faster than control cells (Supplementary Fig S4a). Cell cycle analysis showed that significantly more Oct4 infected cells were in S/G₂-M phases than control cells (43% vs 19%, Supplementary Fig.S4b), supporting that these cells are more proliferative. Oct4-infected cells formed significantly larger colonies in the soft agar assay than the control cells (Fig.1c). When the same number of freshly disassociated WM35GFP or WM35OCT4 cells was incubated in the presence of various concentrations of cisplatin for 24 hours, significantly more *Oct4* infected cells survived cisplatin treatment compared to the control cells. At 1 μ M cisplatin; $16.3 \pm 2.33 \times 10^4$ WM35OCT4 cells survived vs. $4.9 \pm 0.48 \times 10^4$ control cells ($p < 0.001$); and at 10 μ M $3.6 \pm 0.61 \times 10^4$ WM35OCT4 cells survived vs. $0.8 \pm 0.23 \times 10^4$ for control cells ($P < 0.01$). In addition, the control cells did not survive 25 μ M cisplatin treatments, whereas $1.2 \pm 0.36 \times 10^4$ of WM35OCT4 cells survived the high concentration (Fig.1d). Similar results were seen in Oct4 infected WM115A (115AOCT4) cells (see Supplementary Information Fig. S3b). Increased resistance to cisplatin was associated with decreased expression of caspase-3 after cisplatin treatment (see Supplementary information Fig. S3c). Since low oxygen tension promotes survival of stem cells (Morrison et al. 2000), we cultured these cells under 1% O₂ conditions for 24-48 hours. We found that *Oct4* infected cells proliferated significantly better than control cells under hypoxic conditions (Fig.1e).

Increased tumorigenicity and metastatic capacity after Oct4 induced dedifferentiation

We performed a series of xenograft experiments in NOD/SCID Il2rg^{-/-} mice (NSG) in order to study the effect of *Oct4* mediated dedifferentiation *in vivo*. We used WM35 cells in these experiments because it is a well characterized cell line derived from radial growth phase (RGP) of primary melanoma and is known to be incapable of metastasis. Groups of mice (n = 6) were transplanted with replicate inocula of disassociated WM35 or WM35OCT4 cells (2×10^6) on the flank subcutaneously (s.c.), and were then monitored for tumor growth. The xenografts were examined by histology and immunohistochemistry. Due to the large tumor burden of WM35OCT4 xenografts, all the mice were sacrificed 5 weeks after inoculation and necropsy was performed. The tumors formed by WM35OCT4 cells were on average 3 times the size of tumors formed by WM35, (2.8 ± 0.794 g vs 0.60 ± 0.133 g, $P = 0.039$; Fig.2a). The tumors formed by WM35OCT4 cells had significantly higher Ki67 labeling index than that in control tumors (see Supplementary Information Fig. S4c), and they showed diverse cellular morphology characteristic of melanoma tissue (Fig. 2b). In contrast, the WM35 xenografts were composed of tumor cells with uniform morphology. *Oct4* dedifferentiated cells retained Oct4 expression, but the expression of melanocytic markers such as Melan-A (*MLANA*) and S-100 (data not shown) were significantly reduced

(Fig. 2b). Although there was no apparent trigeriminal differentiation such as bone or nerve tissue formation in the Oct4 xenografts, immunohistochemical stains showed that these xenografts expressed markers for ectoderm (pan-cytokeratin and neural filament), mesoderm (actin, muscle specific, clone HHF35) and endoderm (caudal type homeobox 2 (*CDX2*) and podoplanin (*PDPN*)) (Fig.2c).

The primary xenografts were enzymatically dissociated and 1×10^5 cells were injected s.c. into flanks of naïve NSG mice (6 mice per group) in order to establish secondary xenografts. Xenografted NSG mice were followed for 6 weeks, tumors were excised and necropsy was performed. Similar to the primary xenografts, the secondary xenografts formed by WM35OCT4 cells were significantly larger compared to control cells (Fig.2d). The tumor cells isolated from the xenografts maintained their sphere forming capacity (data not shown). These findings demonstrate that dedifferentiated cells have greater tumorigenicity as compared to differentiated melanoma cells.

To test whether *Oct4* dedifferentiation increases metastatic capacity of these cells, we performed tail vein injection assays. Cells (1×10^5) of WM35GFP or WM35OCT4 were injected into NSG mice (n = 5 per group) *i.v.* These mice were followed for 12 weeks and then sacrificed. All the major organs were removed and examined histologically. Similar to previous reports, mice injected with WM35GFP cells did not form any tumor masses in the lung or other major organs. However, we found small tumor islands in the lung of all five mice injected with WM35OCT4 cells, ranging from 0.05 –0.40 mm with an average of 0.14 ± 0.07 mm (Fig.2e). These data indicate that the dedifferentiated cells have acquired the ability to survive and proliferate in the lung.

To dissect the underlying mechanism of this apparent increased metastatic capacity in the lung, we first analyzed the cell migratory capacity of control and WM35OCT4 cells. We performed wound healing assays and showed the wound formed by WM35 cells completely healed after 48 hours, whereas WM35OCT4 cells showed little motility (Supplementary Fig. S5). Migrating cells were characterized by their polymerized actin-based membrane protrusions (Pollard and Borisy 2003). The WM35 cells clearly showed the F-actin staining at the plasma membrane, consistent with their invasion activity. However, the WM35OCT4 cells did not show actin-based membrane protrusions (Fig.3a, left panel). The result was further supported by examination of secreted matrix metalloproteinases 2 (MMP2) using in-gel gelatin zymography, which showed significant loss of MMP2 secretion in the dedifferentiated cells (Fig.3a, right panel). Taken together, these data indicate that increased metastatic capacity of dedifferentiated cells is not due to their enhanced migratory ability but likely results from their increased ability to survive and proliferate in a non-orthotopic environment.

Dedifferentiation is associated with CSC phenotypes

It has been postulated that CSCs share many characteristics with normal stem cells (Lobo et al. 2007). We examined whether *Oct4* increases the CSC characteristics of melanoma cells. To do this, we first performed differentiation assays as previously described (Yu et al. 2009). WM35 or WM35OCT4 cells were cultured in either osteogenic, adipogenic or smooth muscle differentiation medium for 2-3 weeks, and then these cells were examined

for expression of specific differentiation markers. After differentiation, WM35OCT4 cells expressed osteocalcin (*BGLAP*), fatty acid binding protein 4, adipocyte (*FABP-4*) and smooth muscle actin (*ACTG2*) indicative of bone, fat and smooth muscle differentiation, respectively. In contrast, WM35 cells did not express any of these proteins (Fig.3b) after differentiation. Similar results were seen in 115AOCT4 cells (data not shown). To test self-renewal capacity of Oct4 infected cells, we performed limiting dilution assays and single cells were followed for colony formation capacity. In Oct4 expressing cells, the percentage of colony-forming cells increased significantly from $20.7 \pm 6.18\%$ to $61.9 \pm 3.22\%$ ($P < 0.001$), indicating that *Oct4* significantly increases self-renewal capacity of these tumor cells (Fig.3c). Another measure of the CSC is the expression of CSC phenotypic markers such as CD133 (*PROM1*), ATP-binding cassette, sub-family G (WHITE), member 2 (*ABCG2*) (Monzani et al. 2007), ATP-binding cassette, sub-family B (MDR/TAP), member 5 (*ABCB5*) (Schatton et al. 2008), and CD271 (*NGFR*) (Boiko et al. 2010). Quantitative real time RT-PCR analysis showed that WM35OCT4 cells expressed significantly higher level of *ABCG2* and *ABCB5* in comparison to WM35 cells (Fig.3c). However, *CD133* levels were not increased (data not shown). Western blot analysis showed that *ABCB5* protein expression was also significantly increased in WM35, 115A and 3525A cells after *Oct4* infection. In addition, immunohistochemical analysis of the xenografts also confirmed that *ABCB5* protein expression was increased in *Oct4* dedifferentiated cells (Fig.3d). Similarly, *CD271* expression was also significantly increased in WM35 and 115A melanoma cells after Oct4 infection (Fig.3e).

Mechanism underlying Oct4 induced dedifferentiation

To dissect the molecular events that lead to *Oct4* induced dedifferentiation in melanoma cells, we examined whether expression levels of other transcription factors involved in somatic cell reprogramming are altered in WM35OCT4 cells. Quantitative RT-PCR data showed that expression levels of endogenous *Oct4*, *Nanog* and *Klf4* were significantly increased. However, *Rex1*, which has recently been shown to be an essential indicator for pluripotency (Chan et al. 2009), was not increased (Fig.4a), nor was the expression level of *Lin28* (data not shown). To study the effect of *Oct4* expression on mRNA stability, we incubated WM35OCT4 and WM793 cells with Actinomycin D to block transcription and found that *Oct4* expression did not affect *Nanog* mRNA stability in these cells (Supplementary Fig 6). To study *Oct4* promoter activity in dedifferentiated cells, we performed Oct4 luciferase promoter assays and the results showed that *Oct4* promoter activity was significantly elevated in WM35OCT4 cells as compared to WM35 control cells (Fig.4b). These data suggest that dedifferentiation is induced by increased expression of endogenous Oct4 and other reprogramming factors.

Since acquired CSC phenotypes may involve epithelial-mesenchymal transition (EMT) (Mani et al. 2008), we examined the expression of E-Cadherin (*CDH1*) and N-Cadherin (*CDH2*) in the WM35OCT4 cells by western blot. We found that WM35OCT4 cells did not express E-Cadherin, and N-Cadherin levels were down-regulated comparing to control cells (Fig. 4c), suggesting that *Oct4* induced dedifferentiation does not involve EMT.

Because somatic cell reprogramming is associated with *Oct4* promoter demethylation (Takahashi and Yamanaka 2006), we performed bisulfite sequencing analysis (Li et al. 2009) in order to measure the extent to *Oct4* promoter methylation in control and dedifferentiated cells. Significant alteration in *Oct4* promoter methylation in WM35 or WM115A cells was not detected (data not shown). We performed global gene expression profiling studies comparing the dedifferentiated cells (WM35OCT4, WM115AOCT4 and WM3523A) with their parental cells (WM35, WM115A and WM3523A) using Human v2 expression BeadChips (Illumina). We identified 660 probes where the mean expression levels were significantly different between the two groups. Using the top 100 probes, based on the unadjusted P-values, an unsupervised cluster analysis distinguished the samples of dedifferentiated cells from the samples of the parent cells (Fig.4d). To gain insight into the biological processes associated with the 660 probes, we analyzed the list using the National Institute of Allergy and Infectious Diseases/National Institutes of Health Database for Annotation, Visualization and Integrated Discovery (DAVID) Bioinformatics Resource 2008. In the dedifferentiated cell samples, the biological processes for the top two annotation clusters of enriched probes (see Supplementary Information Table S2) were related to transcription and regulation of transcription (enrichment scores of 3.94 and 3.41, respectively). This analysis suggests that dedifferentiation is mediated through regulation of other transcription factors by *Oct4*.

Oct4 is required for CSC phenotypes

To study whether expression of *Oct4* is required to maintain the CSC-like phenotype after dedifferentiation, we knocked down *Oct4* expression in the dedifferentiated WM35OCT4 cells with *Oct4* shRNA. WM35OCT4 cells infected with vector containing scramble shRNA were used as control. As expected, *Oct4* shRNA significantly decreased the *Oct4* expression at both mRNA (data not shown) and protein levels (Fig.5a). After *Oct4* knockdown, the colony size in soft agar was significantly decreased (Fig.5b). In addition, these tumor cells grew slower compared to the control under normoxia (Fig. 5c) and they were significantly less tolerable to hypoxic insult (Fig.5d). *Oct4* knockdown also decreased their resistance to cytotoxic effect of cisplatin (Fig.5e). These data suggest that *Oct4* expression is required for maintaining the CSC-like phenotypes.

Transmembrane Oct4 protein induces dedifferentiation

To study whether transient presence of Oct4 protein may induce similar dedifferentiation, we first construct Oct4 proteins with a His-tag and a cell membrane permeable domain (PTD-OCT4). A GFP protein with a cell membrane permeable domain was used as a control. We incubated WM35 cells with PTD-OCT4 in the presence or absence of valproic acid. The tumor cells were treated 4 times with the protein during a 10 day period. The presence of the exogenous Oct4 protein was visualized with an antibody against His-tag (Fig.6a, upper panel) at day 10. Morphological changes occurred slower in these cells than in tumor cells infected with viruses carrying Oct4. Sphere formation started two weeks after the treatment (Fig.6b). Quantitative real time RT-PCR showed that there was a significant decrease in expression of melanocytic markers microphthalmia-associated transcription factor (*MITF*) and tyrosinase (*TYR*) comparing to melanocytes or control WM35 cells. (Fig. 6c). The levels of endogenous Oct4, Nanog and KLF-4 gene expression were comparable to

hEC cells (Fig.6d). In addition, these cells were significantly more resistant to cisplatin induced cytotoxicity than control cells (Fig.6e). The control protein treated cells did not show any changes. Morphological changes occurred only in cells treated with the Oct4 proteins in the presence of valproic acid. Valproic acid is a histone deacetylase (HDAC) inhibitor and it is known to facilitate somatic reprogramming. These data showed for the first time that Oct4 protein alone can induce tumor cell dedifferentiation, and indicate that transient Oct4 expression with concomitant histone acetylation is sufficient to activate endogenous dedifferentiation pathways.

Oct4 expression is regulated by hypoxia

It has been shown that Oct4 is regulated by hypoxia inducible factors (HIFs) in a transgenic mouse model (Covello et al. 2006). We examined whether Oct4 expression is regulated by hypoxia in melanoma cells. We incubated WM793 cells under 1% or room O₂ and then the cells were snap frozen for further processing. Hypoxia significantly increased *Oct4* gene expression using quantitative RT-PCR (Fig. 7a) and protein expression using western blot analysis (Fig. 7b). To study whether hypoxia affects localization of Oct4, we incubated WM35OCT4 cells under hypoxia for 0, 4 and 16 hours, and found that hypoxia did not change the nuclear localization of Oct4 (Supplementary Fig. 7).

Oct4 is expressed in melanoma tissue

To study whether Oct4 plays a potential role during melanoma progression, we first examined *Oct4* gene expression in fresh metastatic melanoma tissues. The protocol has been approved by the University of Pennsylvania Institutional Review Board. Four of five melanomas expressed detectable *Oct4* gene (Fig.7c). To confirm the expression of Oct4 in the tissue, we performed Oct4 immunohistochemical stain and found that a small population of tumor cells showed nuclear staining for Oct4 (Fig.7d). Positive cells can be detected in 18 of 30 vertical growth phase or metastatic melanomas whereas they were not seen in the radial growth phase of any primary melanomas. The Oct4 positive cells were distributed unevenly in the tissue and some were near necrotic areas.

Discussion

In this study, we demonstrate that forced expression of *Oct4* alone is sufficient to dedifferentiate melanoma cells to CSC-like cells, and intermittent exposure to Oct4 protein has a similar effect. Dedifferentiation of melanoma cells is associated with reactivation of other embryonic transcription factors. These data suggest that Oct4 is a positive regulator of melanoma cell dedifferentiation.

It is well known that lower stage of tumor differentiation such as in neuroblastoma and in breast cancer is linked to poor prognosis (Helczynska et al. 2003; Jogi et al. 2002). Dedifferentiated glioma cancer cells showed strong drug resistance and they expressed increased neural stem cell related genes (Kang et al. 2006). CD271⁺ melanoma CSCs had a dedifferentiated phenotype as they lost expression of common melanocytic markers (Boiko et al. 2010). Our data show that during Oct4 induced dedifferentiation, the melanoma cells also lose melanocytic marker expression. Although loss of pigmentation is commonly seen

during melanoma progression, some highly aggressive melanomas are heavily pigmented, suggesting that dedifferentiation is only one of the mechanisms that may lead to aggressive tumor behavior.

Tumor cells are more susceptible for Oct4 induced dedifferentiation than normal cells. Our study showed that *Oct4* has little effect on normal melanocytes, whereas it induces dramatic changes in melanoma cells. This result is consistent with a prior study which shows that aberrant activation of *Oct4* in epithelium results in dysplastic proliferation, and the target cells of *Oct4*-induced dysplasia are epithelial progenitor/stem cells rather than differentiated squamous cells (Hochedlinger et al. 2005). It was surprising that transmembrane Oct4 protein alone was able to induce dedifferentiation as virally delivered Oct4. To our knowledge, this is the first study to show that transient and intermittent exposure to Oct4 protein alone is sufficient to induce human cell dedifferentiation. The efficient dedifferentiation of melanoma cells is likely resulted from their endogenous expression of *Sox2*, *c-Myc*, and *Klf4*. Endogenous expression of reprogramming factors has been attributed to the *Oct4* induced reprogramming of neural stem cells to iPS cells (Kim et al. 2009a; Kim et al. 2009b). These data suggest that the embryonic transcription factor circuitry in the melanoma cells is at least partially active, allowing efficient dedifferentiation of melanoma cells by Oct4.

There is a controversy surrounding melanoma CSCs. ABCB5 and CD271 have been shown as markers for a rare population of melanoma initiating cells (Schatten et al. 2008; Boiko et al. 2010). However, Morrison and colleagues showed that over 25% of single melanoma cells obtained directly from patients formed tumors in NOD/SCID IL2R γ (null) mice, suggesting that majority of melanoma cells are tumorigenic (Quintana et al. 2008; Quintana et al. 2010). Therefore, we did not perform single cell xenograft assay to test tumorigenicity of the dedifferentiated cells, but rather examined their tumorigenicity and their capacity to survive in heterotopic environment. Our results showed that the Oct4-dedifferentiated cells are more tumorigenic in the subcutis and in the lung, and they have acquired CSC-like phenotypes, suggesting that CSC phenotype is a dynamic process. More recently, Herlyn and colleagues showed that a subpopulation of JARID1B positive melanoma cells is required for continuous tumor growth and expression of JARID1B is dynamically regulated, indicating that melanoma maintenance is mediated by a temporarily distinct subpopulation (Roesch et al. 2010). Thus, these data demonstrate phenotypic plasticity of melanoma cells and suggest that CSC phenotypes may be temporarily regulated.

Expression of endogenous Oct4 in tumor cells may be regulated by its microenvironment. Oct4 is a known target of hypoxia inducible factor (HIF)-2 α (Covello et al. 2006). It has been shown that brain cancer cells express higher levels of *Oct4*, *Nanog* and *Klf4* under hypoxic condition (Li and Rich 2010). Our result confirmed that Oct4 expression in melanoma is increased under hypoxia. In the melanoma tissues, we found that only a minor subpopulation of melanoma cells expresses Oct4 and the distribution of these cells within the melanoma tissues is not uniform. Because we only examined one stained section from each melanoma, the uneven distribution of antigen may explain that Oct4 positive cells were found in only 60% of melanomas examined in this study. Since our data showed that transient expression of Oct4 protein is sufficient to induce dedifferentiation of melanoma

cells and Oct4 can be regulated by hypoxia, we speculate that Oct4 may mediate certain effects of hypoxia on tumor progression. Nevertheless, more studies are needed to elucidate the regulation and function of Oct4 in cancer. In conclusion, our data support that Oct4 is a positive regulator of tumor dedifferentiation and suggest that CSC phenotypes can be acquired through dedifferentiation.

Materials and methods

Cell Culture, plasmids and lentiviral production

Human melanoma cell lines (WM35, WM793, WM9, 115A, 3523A and 1205Lu) were cultured in 2% MCDB or hESCM4 medium under normoxic or hypoxic conditions as previously described (Yu et al. 2009; Kumar et al. 2007). Lentiviral vectors (pSin-EF2-Oct4-Pur, Addgene plasmid 16579; vexGFP_2A_OCT4, Addgene plasmid 22240; shRNA to Oct4, a generous gift from Dr. GQ Daley (Zaehres et al. 2005)) was co-transfected into 293T cells with packing vector (pCMV 8.2 dupr and pCMV VSVG), and viral supernatants were collected 48 and 72 h post transfection. *Oct4* promoter-Luc construct was purchased from Addgene (Addgene plasmid 17221).

In vitro differentiation and Immunofluorescence

The differentiation assay was performed using human mesenchymal stem cell functional identification kit (R&D systems) and immunofluorescence study was performed as previous described (Yu et al. 2009). Cells were imaged with a Leica Inverted fluorescence microscope with a Leica camera.

Subcutaneous xenograft and tail vein injection assays

WM35 and WM35OCT4 cells (2×10^6) were injected subcutaneously into NOD/SCID Il2rg^{-/-} mice (6 mice per group). The protocol has been approved by University of Pennsylvania Institutional Animal Care and Use Committee. Tumor cells (1×10^5) from the primary xenografts were enzymatically dissociated and inject subcutaneously into naïve NOD/SCID Il2rg^{-/-} mice (6 mice per group) for secondary xenografts. 1×10^5 cells of WM35 or WM35OCT4 cells were injected into the tail vein of NOD/SCID Il2rg^{-/-} mice (5 mice per group) and these mice were sacrificed 12 weeks later for necropsy and histological examination.

Construction of membrane permeable Oct4 protein and dedifferentiation induction

The cell membrane permeable OCT4 construct PTD-OCT4 containing a PTD peptide similar to the transduction domain of HIV TAT protein (Zhou et al. 2009). Briefly, OCT4 (a.a. 1-360, Gene ID: 5460 POU5F1, accession# NM_002701.4) was amplified and PTD-OCT4 cDNA was cloned into the pET15b vector for expression in *E. coli*. As a result, the recombinant OCT4 protein contains the His-tag and the PTD domain at the N-terminus of OCT4: MGSSHHHHHSSGLVPRGSHMYGRKKRRQRRR. The fusion proteins were expressed in an BL21 (DE3) codon plus strain and protein isolated and refolded as previously described (Masuda et al. 2006).

Melanoma cells (WM35) were treated with combine recombinant OCT4 protein at the concentration of 8µg/ml with or without 1 mM valproic acid (VPA) in serum free MCDB media. Cells were cultured for additional 36 h to 48 h before repeating the same protein transduction procedure. Three additional protein transduction experiments were performed.

Limiting dilution assays

Melanoma cells expressing OCT4 and control WM35 cells were washed with PBS and trypsinized. The cells were then re-suspended at 100 cells ml⁻¹ in HECM4 media. Cells were then dispensed at 10 µl of cells suspension into 96 well plates containing 90 µl of HECM4 media. The plates were incubated in each well was inspected for cell growth. After another 7days, wells were inspected for colony formation.

Cisplatin treatment

Freshly disassociated melanoma cells were washed with PBS and 1 × 10⁵ cells were seeded in 6 well plates. The plates were incubated at 37 °C for 24 hrs in a humidified CO₂ incubator. The medium was aspirated from the wells and replaced with growth media containing different concentrations of cisplatin (1 µM, 10 µM, 25 µM and 100 µM). After 24 h at 37 °C viable cells were counted by trypan blue dye exclusion. Experiments were carried out in triplicate.

Western blot, alkaline phosphatase staining, immunocytochemistry and immunohistochemistry

Adherent monolayer cells were washed with ice-cold PBS and lysed to analyze analysis total protein. Sphere-forming cells were washed with ice-cold 1 x PBS and then lysed in Tissue Protein Extraction Reagent (T-PER, Pierce, Rockford, IL) with (1 x) Protease Inhibitor cocktail (Sigma) and 1 mmol l⁻¹ phenylmethylsulfonyl fluoride (Sigma). Lysates were homogenized on ice, centrifuged at 10,000 rpm for 5 min and the resultant supernatant was assayed for total protein concentration. Fifty micrograms of proteins were separated in Nu PAGE 4-12% Bis-Tris Gel (Invitrogen) and transferred to a polyvinylidene difluoride (PVDF) membranes (Hybond-P, Amersham Biosciences). Membranes were blocked and then incubated with antibodies against OCT4 (Cell Signaling), ABCB5 (abcam), β-actin (1:2500, Sigma), E-Cadherin (BD Biosciences), or N-Cadherin (ZYMED) in 5% BSA TBST buffer [150 mmol/L Tris-HCl (pH 8), 150 mmol l⁻¹ NaCl, 5% BSA, and 0.1% Tween 20]. The membranes were washed thrice with wash buffer for 5 min and incubated with horseradish peroxidase-conjugated secondary antibodies and washed again before being processed with chemiluminescence reagents (ECL Western Blotting Detection System, Amersham Biosciences). Bands were scanned and quantified using a ChemiDoc XRS system (Bio-Rad Laboratories, Hercules, CA).

For F-actin staining, cells were washed with PBS and fixed with fixing buffer (3.7% formaldehyde, 10mM HEPES and 0.1M NaCl) for 12 min. The cells were then incubated in 50 mM glycine/PBS for 10 min, permeabilized in PBST for 5 min, blocked for 10 min with 2% BSA in PBST, and then incubated with Alexa 488-phalloidin (Invitrogen) to stain for F-actin.

Immunohistochemical assays were performed on 5 μ m thick formalin-fixed paraffin embedded sections. Slides were incubated with the antibodies against podoplanin (Signet Laboratories, Dedham, MA); neurofilament (a kind gift from Dr. Virginia Lee), PanCK (Dako), CDX2 (BioGenex, San Ramone, CA) and HHF-35 (Thermo Scientific). Immunohistochemical staining was performed on a DakoCytomation Autostainer using the EnVision+ HRP DAB system (DakoCytomation) according to manufacturer's recommendations. Positive and negative controls were performed in each run.

RNA Stability Assay

The half-life of *Nanog* mRNA was determined by treating WM35OCT4 or WM793 cells with Actinomycin D (10 μ g/ml) in the growth medium to block transcription. The cells were harvested every 2 hrs (0, 2, 4, 6 hr) and processed for total RNA. *Nanog* and β -*actin* gene expression at each time point was measured by quantitative RT-PCR.

Global gene expression analysis and data processing

For transcriptome profiling, 400 ng of total DNA-free RNA was used as input for labelled cRNA synthesis (Illumina TotalPrep RNA Amplification Kit, Ambion) following the manufacturer's instructions. Quality-checked cRNA samples were hybridized onto HumanRef-8 v2 expression BeadChips (Illumina) using protocols suggested by the manufacturer.

The least variant set (LVS) method was used to normalize the gene expression values. The analysis included 12,445 probes of the 48,701 probes on the array. A probe was included when its expression in the 6 samples had adequate variability (i.e. the difference between its maximum and minimum of the 6 sample values was greater than 100) where the difference between the two groups would be potentially meaningful. A two-sample *t*-test with Satterwaithe's adjustment when the two sample variances were unequal was used to test for differences in gene expression between the dedifferentiated cell and parent cells after transformation of the gene expression values using the logarithm.

Statistical analyses

The data represent mean \pm s.e.m values. The effect of treatments and differences among experimental groups were assessed using analysis of variance (ANOVA) and appropriate post-hoc test. The differences between two experimental groups were determined using Student's *t*-tests. A two-tailed value of $P < 0.05$ was considered statistically significant.

Supplementary Material

Refer to Web version on PubMed Central for supplementary material.

Acknowledgements

We thank Dr. M. Herlyn (The Wistar Institute) for providing the melanoma cell lines; Dr. GQ Daley (Harvard) for providing shRNA to Oct4; Dr. W. Lee (University of Pennsylvania) for suggestions to the manuscript; the histology laboratory at the Department of Pathology and Laboratory Medicine for assistance in histological studies; and Drs. K Huang and JS Martin for manuscript editing.

This work was supported by the grants AR-054593, CA-116103 and CA-093372 from National Institute of Health to XX.

Reference List

- Ben-Porath I, Thomson MW, Carey VJ, Ge R, Bell GW, Regev A, Weinberg RA. An embryonic stem cell-like gene expression signature in poorly differentiated aggressive human tumors. *Nat Genet.* 2008; 40:499–507. [PubMed: 18443585]
- Bennett DC. Differentiation in mouse melanoma cells: initial reversibility and an on-off stochastic model. *Cell.* 1983; 34:445–453. [PubMed: 6616619]
- Boiko AD, Razorenova OV, van de RM, Swetter SM, Johnson DL, Ly DP, et al. Human melanoma-initiating cells express neural crest nerve growth factor receptor CD271. *Nature.* 2010; 466:133–137. [PubMed: 20596026]
- Chan EM, Ratanasirintrao S, Park IH, Manos PD, Loh YH, Huo H, et al. Live cell imaging distinguishes bona fide human iPS cells from partially reprogrammed cells. *Nat Biotechnol.* 2009; 27:1033–1037. [PubMed: 19826408]
- Chen Y, Shi L, Zhang L, Li R, Liang J, Yu W, Sun L, Yang X, Wang Y, et al. The molecular mechanism governing the oncogenic potential of SOX2 in breast cancer. *J Biol Chem.* 2008; 283:17969–17978. [PubMed: 18456656]
- Chen Z, Xu WR, Qian H, Zhu W, Bu XF, Wang S, et al. Oct4, a novel marker for human gastric cancer. *J Surg Oncol.* 2009; 99:414–419. [PubMed: 19347886]
- Covello KL, Kehler J, Yu H, Gordan JD, Arsham AM, Hu CJ, et al. HIF-2alpha regulates Oct-4: effects of hypoxia on stem cell function, embryonic development, and tumor growth. *Genes De.* 2006; 20:557–570.
- Daley GQ. Common themes of dedifferentiation in somatic cell reprogramming and cancer. *Cold Spring Harb Symp Quant Biol.* 2008; 73:171–174. 2008. [PubMed: 19150965]
- Dimos JT, Rodolfa KT, Niakan KK, Weisenthal LM, Mitsumoto H, Chung W, et al. Induced pluripotent stem cells generated from patients with ALS can be differentiated into motor neurons. *Science.* 2008; 321:1218–1221. [PubMed: 18669821]
- Gabbert H, Wagner R, Moll R, Gerharz CD. Tumor dedifferentiation: an important step in tumor invasion. *Clin Exp Metastasis.* 1985; 3:257–279. [PubMed: 3907917]
- Hanna J, Saha K, Pando B, van ZJ, Lengner CJ, Creighton MP, et al. Direct cell reprogramming is a stochastic process amenable to acceleration. *Nature.* 2009; 462:595–601. [PubMed: 19898493]
- Hanna J, Wernig M, Markoulaki S, Sun CW, Meissner A, Cassady JP, et al. Treatment of sickle cell anemia mouse model with iPS cells generated from autologous skin. *Science.* 2007; 318:1920–1923. [PubMed: 18063756]
- Helczynska K, Kronblad A, Jogi A, Nilsson E, Beckman S, Landberg G, Pahlman S. Hypoxia promotes a dedifferentiated phenotype in ductal breast carcinoma in situ. *Cancer Res.* 2003; 63:1441–1444. [PubMed: 12670886]
- Hochedlinger K, Yamada Y, Beard C, Jaenisch R. Ectopic expression of Oct-4 blocks progenitor-cell differentiation and causes dysplasia in epithelial tissues. *Cell.* 2005; 121:465–477. [PubMed: 15882627]
- Hu L, McArthur C, Jaffe RB. Ovarian cancer stem-like side-population cells are tumorigenic and chemoresistant. *Br J Cancer.* 2010; 102:1276–1283. [PubMed: 20354527]
- Hu T, Liu S, Breiter DR, Wang F, Tang Y, Sun S. Octamer 4 small interfering RNA results in cancer stem cell-like cell apoptosis. *Cancer Res.* 2008; 68:6533–6540. [PubMed: 18701476]
- Jogi A, Ora I, Nilsson H, Lindeheim A, Makino Y, Poellinger L, et al. Hypoxia alters gene expression in human neuroblastoma cells toward an immature and neural crest-like phenotype. *Proc Natl Acad Sci U S A.* 2002; 99:7021–7026. [PubMed: 12011461]
- Kang SK, Park JB, Cha SH. Multipotent, dedifferentiated cancer stem-like cells from brain gliomas. *Stem Cells Dev.* 2006; 15:423–435. [PubMed: 16846378]
- Kawamura T, Suzuki J, Wang YV, Menendez S, Morera LB, Raya A, et al. Linking the p53 tumour suppressor pathway to somatic cell reprogramming. *Nature.* 2009; 460:1140–1144. [PubMed: 19668186]

- Kim JB, Greber B, rauzo-Bravo MJ, Meyer J, Park KI, Zaehres H, Scholer HR. Direct reprogramming of human neural stem cells by OCT4. *Nature*. 2009a; 461:649–3. [PubMed: 19718018]
- Kim JB, Sebastiano V, Wu G, rauzo-Bravo MJ, Sasse P, Gentile L, et al. Oct4-induced pluripotency in adult neural stem cells. *Cell*. 2009b; 136:411–419. [PubMed: 19203577]
- Kumar SM, Yu H, Edwards R, Chen L, Kazianis S, Brafford P, et al. Mutant V600E BRAF increases hypoxia inducible factor-1alpha expression in melanoma. *Cancer Res*. 2007; 67:3177–3184. [PubMed: 17409425]
- Li W, Zhou H, Abujarour R, Zhu S, Young JJ, Lin T, et al. Generation of human-induced pluripotent stem cells in the absence of exogenous Sox2. *Stem Cells*. 2009; 27:2992–3000. [PubMed: 19839055]
- Li Z, Rich JN. Hypoxia and hypoxia inducible factors in cancer stem cell maintenance. *Curr Top Microbiol Immunol*. 2010; 345:21–30. [PubMed: 20582533]
- Liu T, Xu F, Du X, Lai D, Liu T, Zhao Y, et al. Establishment and characterization of multi-drug resistant, prostate carcinoma-initiating stem-like cells from human prostate cancer cell lines 22RV1. *Mol Cell Biochem*. 2010; 340:265–273. [PubMed: 20224986]
- Lobo NA, Shimono Y, Qian D, Clarke MF. The biology of cancer stem cells. *Annu Rev Cell Dev Biol*. 2007; 23:675–699. [PubMed: 17645413]
- Magnifico A, Albano L, Campaner S, Delia D, Castiglioni F, Gasparini P, et al. Tumor-initiating cells of HER2-positive carcinoma cell lines express the highest oncoprotein levels and are sensitive to trastuzumab. *Clin Cancer Res*. 2009; 15:2010–2021. [PubMed: 19276287]
- Mani SA, Guo W, Liao MJ, Eaton EN, Ayyanan A, Zhou AY, et al. The epithelial-mesenchymal transition generates cells with properties of stem cells. *Cell*. 2008; 133:704–715. [PubMed: 18485877]
- Masuda K, Richter M, Song X, Berezov A, Masuda K, Murali R, et al. AHNP-streptavidin: a tetrameric bacterially produced antibody surrogate fusion protein against p185her2/neu. *Oncogene*. 2006; 25:7740–7746. [PubMed: 16785990]
- Monzani E, Facchetti F, Galmozzi E, Corsini E, Benetti A, Cavazzin C, et al. Melanoma contains CD133 and ABCG2 positive cells with enhanced tumourigenic potential. *Eur J Cancer*. 2007; 43:935–946. [PubMed: 17320377]
- Morrison SJ, Csete M, Groves AK, Melega W, Wold B, Anderson DJ. Culture in reduced levels of oxygen promotes clonogenic sympathoadrenal differentiation by isolated neural crest stem cells. *J Neurosci*. 2000; 20:7370–7376. [PubMed: 11007895]
- Park IH, Arora N, Huo H, Maherali N, Ahfeldt T, Shimamura A, et al. Disease-specific induced pluripotent stem cells. *Cell*. 2008; 134:877–886. [PubMed: 18691744]
- Peng S, Maihle NJ, Huang Y. Pluripotency factors Lin28 and Oct4 identify a sub-population of stem cell-like cells in ovarian cancer. *Oncogene*. 2010; 29:2153–2159. [PubMed: 20101213]
- Pollard TD, Borisy GG. Cellular motility driven by assembly and disassembly of actin filaments. *Cell*. 2003; 112:453–465. [PubMed: 12600310]
- Quintana E, Shackleton M, Foster HR, Fullen DR, Sabel MS, Johnson TM, Morrison SJ. Phenotypic heterogeneity among tumorigenic melanoma cells from patients that is reversible and not hierarchically organized. *Cancer Cell*. 2010; 18:510–523. [PubMed: 21075313]
- Quintana E, Shackleton M, Sabel MS, Fullen DR, Johnson TM, Morrison SJ. Efficient tumour formation by single human melanoma cells. *Nature*. 2008; 456:593–598. [PubMed: 19052619]
- Roesch A, Fukunaga-Kalabis M, Schmidt EC, Zabierowski SE, Brafford PA, Vultur A, et al. A temporarily distinct subpopulation of slow-cycling melanoma cells is required for continuous tumor growth. *Cell*. 2010; 141:583–594. [PubMed: 20478252]
- Saigusa S, Tanaka K, Toiyama Y, Yokoe T, Okugawa Y, Ioue Y, et al. Correlation of CD133, OCT4, and SOX2 in rectal cancer and their association with distant recurrence after chemoradiotherapy. *Ann Surg Oncol*. 2009; 16:3488–3498. [PubMed: 19657699]
- Schatton T, Murphy GF, Frank NY, Yamaura K, Waaga-Gasser AM, Gasser M, et al. Identification of cells initiating human melanomas. *Nature*. 2008; 451:345–349. [PubMed: 18202660]
- Schoenhals M, Kassambara A, De VJ, Hose D, Moreaux J, Klein B. Embryonic stem cell markers expression in cancers. *Biochem Biophys Res Commun*. 2009; 383:157–162. [PubMed: 19268426]

- Strizzi L, Abbott DE, Salomon DS, Hendrix MJ. Potential for cripto-1 in defining stem cell-like characteristics in human malignant melanoma. *Cell Cycle*. 2008; 7:1931–1935. [PubMed: 18604175]
- Takahashi K, Tanabe K, Ohnuki M, Narita M, Ichisaka T, Tomoda K, Yamanaka S. Induction of pluripotent stem cells from adult human fibroblasts by defined factors. *Cell*. 2007; 131:861–872. [PubMed: 18035408]
- Takahashi K, Yamanaka S. Induction of pluripotent stem cells from mouse embryonic and adult fibroblast cultures by defined factors. *Cell*. 2006; 126:663–676. [PubMed: 16904174]
- Viswanathan SR, Powers JT, Einhorn W, Hoshida Y, Ng TL, Toffanin S, et al. Lin28 promotes transformation and is associated with advanced human malignancies. *Nat Genet*. 2009; 41:843–848. [PubMed: 19483683]
- Yu H, Kumar SM, Kossenkov AV, Showe L, Xu X. Stem cells with neural crest characteristics derived from the bulge region of cultured human hair follicles. *J Invest Dermatol*. 2009; 130:1227–36. [PubMed: 19829300]
- Yu J, Hu K, Smuga-Otto K, Tian S, Stewart R, Slukvin II, Thomson JA. Human induced pluripotent stem cells free of vector and transgene sequences. *Science*. 2009; 324:797–801. [PubMed: 19325077]
- Zaehres H, Lensch MW, Daheron L, Stewart SA, Itskovitz-Eldor J, Daley GQ. High-efficiency RNA interference in human embryonic stem cells. *Stem Cells*. 2005; 23:299–305. [PubMed: 15749924]
- Zhang X, Han B, Huang J, Zheng B, Geng Q, Aziz F, Dong Q. Prognostic significance of OCT4 expression in adenocarcinoma of the lung. *Jpn J Clin Oncol*. 2010c; 40:961–966. [PubMed: 20462980]
- Zhou H, Wu S, Joo JY, Zhu S, Han DW, Lin T, et al. Generation of induced pluripotent stem cells using recombinant proteins. *Cell Stem Cell*. 2009; 4:381–384. [PubMed: 19398399]

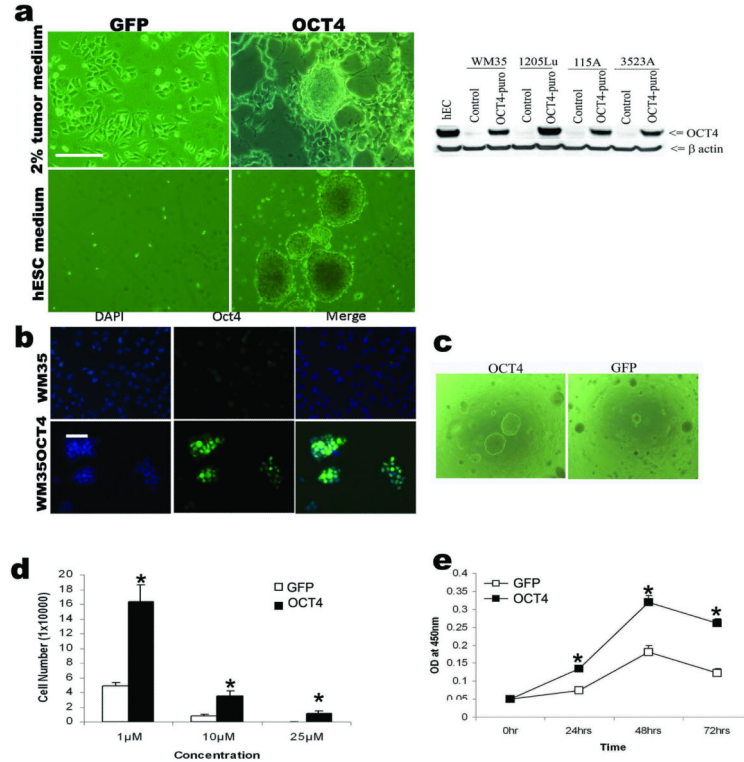


Figure 1. Oct4 induced phenotypic changes in vitro

(a) Morphology of WM35GFP (upper left) and WM35OCT4 cells (upper right) in 2% MCDB tumor medium. WM35GFP cells were not able to survival in the hESCM4 medium (lower left) whereas WM35OCT4 cells formed floating spheroids similar to embryoid body (lower right). Representatives image from 5 independent experiments. Bar indicates 100 μ m. Western blotting showed levels of Oct4 expression in control and Oct4 infected cells. Human EC cells were used as a positive control and β -actin was used as a loading control. Representative images from 3 replicate experiments. (b) Serially passaged WM35 or WM35OCT4 cells were stained with Oct4 by immunocytochemistry and nuclei with DAPI. Bar indicates 50 μ m. (c) Dedifferentiated cells from larger colonies in the soft agar assay. Representative images from 3 replicate experiments. (d) Drug resistance. 1×10^5 tumor cells were seeded in 2% MCDB medium containing 1 μ M, 10 μ M, or 25 μ M cisplatin. Cultured for 24 hours, and cells were stained with trypan blue and counted (n = 3 replicate experiments). * indicates $P < 0.05$ comparing to control cells. (e) 1×10^4 cells were seeded and then cultured under 1% O₂ for 24-72 hours (n = 3 replicate experiments). Cell proliferation was assessed by WTT assay. * indicates $P < 0.05$ comparing experimental to control cells. The data represent mean \pm s.e.m values.

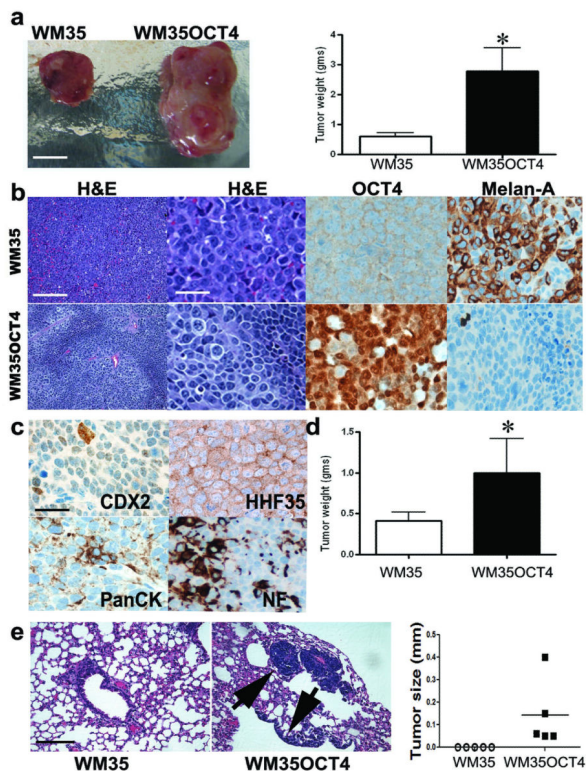


Figure 2. Oct4 induced increase in tumorigenicity in vivo

(a) Two million WM35GFP or WM35OCT4 cells were injected subcutaneously in the flanks of NOD/SCID/IL- γ mice ($n = 6$) and these mice were followed for 5 weeks. Representative primary xenografts were shown in the left and average tumor weight was shown in the right. Bar indicates 1 cm. * indicates $P < 0.05$. (b) Hematoxylin and Eosin (H & E) stain and immunohistochemical stains for Oct4 and Melan-A. Bar in low power view indicates 200 μm , and Bar in high power indicates 40 μm . (c) The dedifferentiated tumor cells expressed markers for Endoderm (CDX2), Mesoderm (HNF35) and Ectoderm (PanCK and neurofilament). Bar indicates 40 μm . (d) 100K cells were isolated from the primary xenografts and directly inject subcutaneously to the flanks of naïve NOD/SCID/IL- γ mice ($n = 6$) to form secondary tumors. Average secondary tumor weight is shown (* $P < 0.05$). (e) 100K tumor cells were injected via tail vein of NOD/SCID/IL- γ mice ($n = 5$) and these mice were followed for 12 weeks. Representative histology of lung in mice received either WM35 or WM35OCT4 cells. All the 5 mice that received WM35OCT4 cells developed tumors in the lung (right panel). Arrows point to the tumor. Bar indicates 200 μm . The data represent mean \pm s.e.m values.

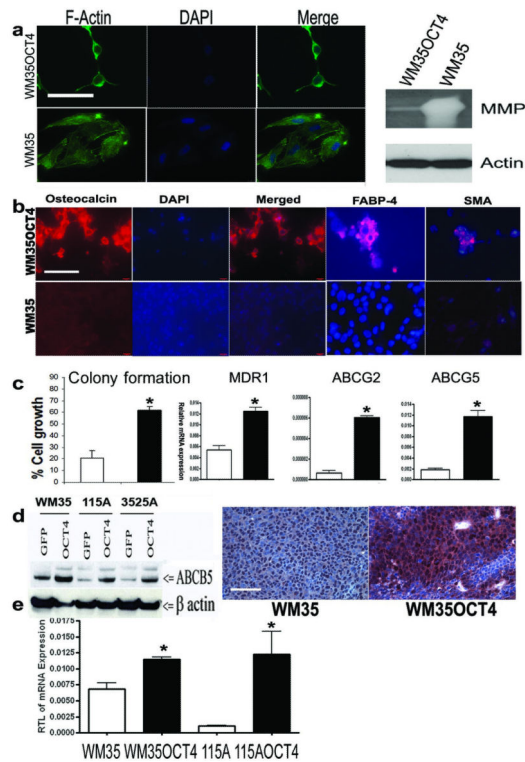


Figure 3. Acquired CSC-like phenotypes

(a) F-actin polymerization in WM35 cells resulted in cell membrane protrusion and migration activity, whereas WM35OCT4 cells did not show any membrane protrusion. Nuclei were stained with DAPI. Bar indicates 40 μm. Secretion of MMP2 from WM35 and WM35OCT4 was examined using MMP2 in-gel gelatin zymography. Actin from cell lysate was used as loading control. (b) Multipotent differentiation. DAPI is used to visualize nuclei. Immunocytochemistry for Osteocalcin, FABP-4 and SMA was performed. Representative images from 3 replicate experiments. Bar indicates 40 μm. (c) Limiting dilution assays were performed to assess self-renewal capacity. The number of colonies formed was counted and averaged in 3 replicate experiments (* $P < 0.01$). Real time quantitative PCR was performed to assess the expression of MDR1, ABCG2 and ABCG5 (n = 3 replicates)(* $P < 0.01$). (d) Western blot showed increased ABCB5 expression in WM35, 115A and 3525A cells after dedifferentiation. Bar indicates 100 μm. (e) Real time quantitative PCR was performed for CD271 (n = 3 replicates) (* $P < 0.01$). The data represent mean \pm s.e.m values.

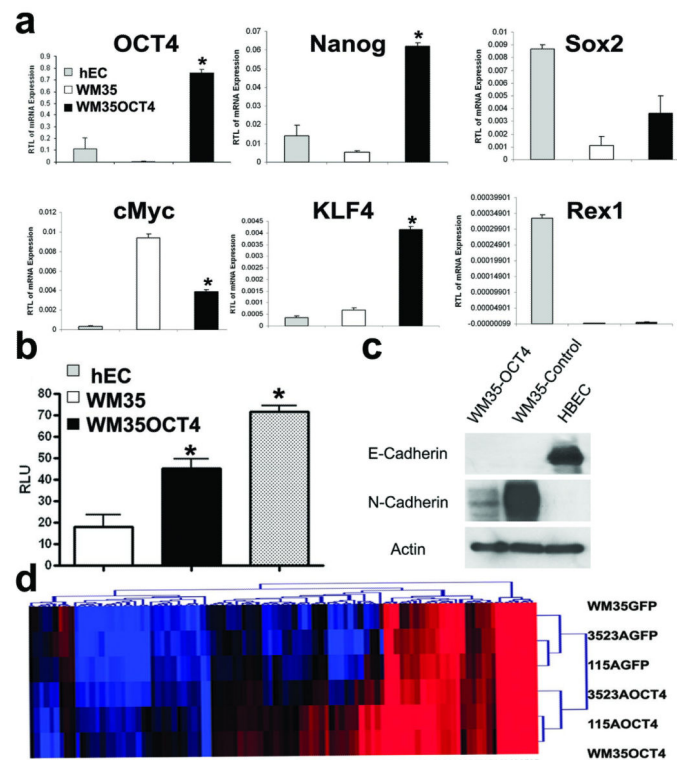
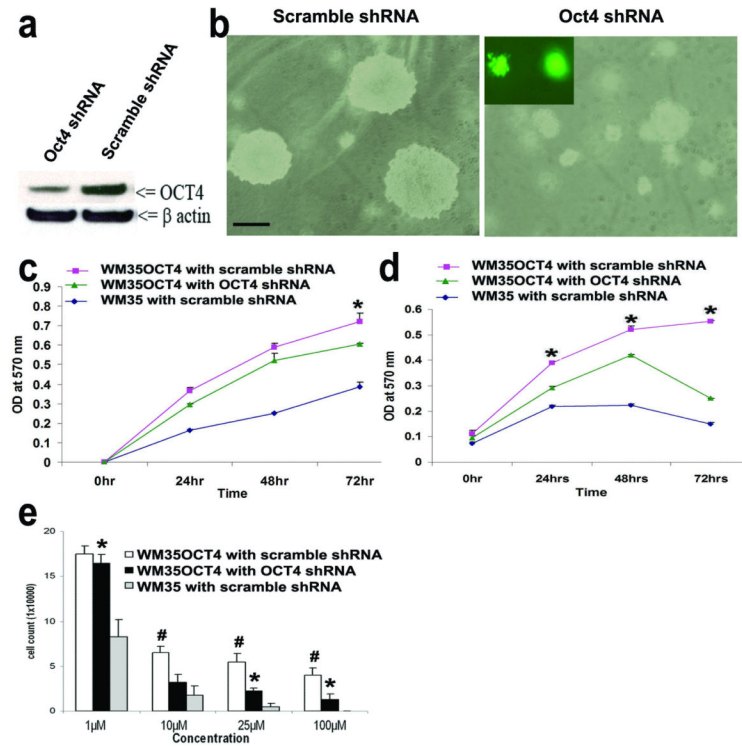


Figure 4. Mechanisms underlying *Oct4* induced dedifferentiation

(a) Quantitative RT-PCR was performed for *Oct4*, *Nanog*, *Sox2*, *cMyc*, *KLF4* and *Rex1* ($n = 3$ replicate experiments) and showed significant increase of *Oct4*, *Nanog* and *KLF4* ($*P < 0.01$). Human EC cells were used as a control. (b) *Oct4* promoter luciferase reporter assay ($n = 3$ replicate experiments). $*P < 0.05$ comparing WM35OCT4 vs WM35. hEC was used as positive control. (c) Cadherin expression. Western blot analysis of E- and N-Cadherin expression after *Oct4* infection. WM35 and WM35OCT4 cells did not express E-Cadherin, and there was down regulation of N-Cadherin in WM35OCT4 cells. Human bronchial epithelial cells were used as controls. (d) Global gene expression profiling was performed. An unsupervised cluster analysis using the top 100 probes significantly changed after dedifferentiation.



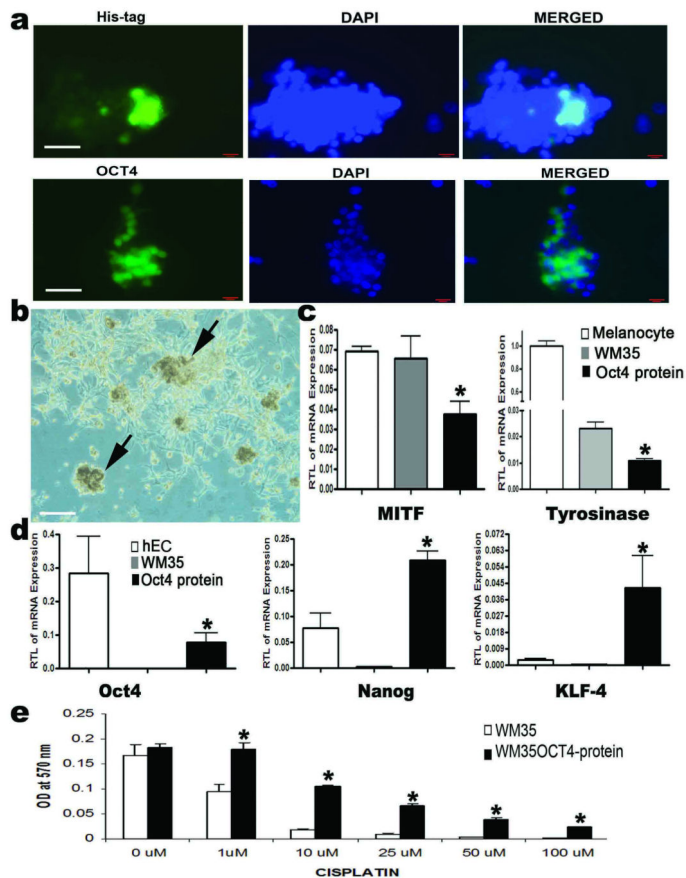


Figure 6. Transmembrane Oct4 protein induces dedifferentiation

(a) The cell membrane permeable PTD-OCT4 protein with a His-tag was used to transduce WM35 cells 4 times in a 10 day period. The presence of exogenous protein was detected by anti-His-tag antibody, and expression of Oct4 was also evident 4 days after the last treatment. Bars indicate 40 μ m. (b) The tumor cells started to form spheres 2 weeks after the last treatment. Arrows points to the spheres. Representatives image from 3 independent experiments. (c) The sphere forming cells expression significantly lower levels of Mitf and tyrosinase gene than normal melanocytes and control WM35 (n= 3 replicates, * $P < 0.01$). (d) Quantitative RT PCR was performed and showed that Oct4, Nanog and Klf-4 expression levels in dedifferentiated cells were similar or higher than in hEC cells. hEC cells were used as a positive control (n = 3 replicate, * $P < 0.05$). WM35 express little of these stemness genes. (e) The Oct4-protein-dedifferentiated cells were more resistant to cisplatin (n = 3 replicate experiments) (* $P < 0.01$). The data represent mean \pm s.e.m values.

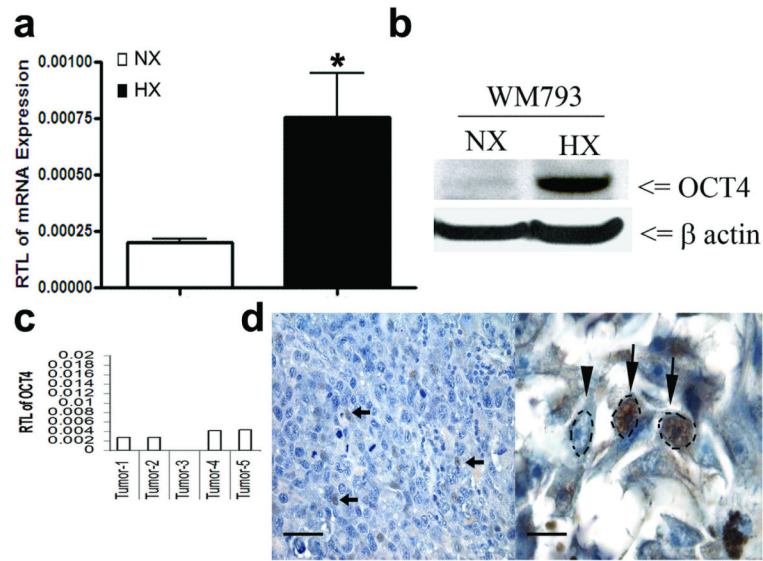


Figure 7. Regulation of Oct4 by hypoxia and Oct4 expression in melanoma tissues
(a) Hypoxia increases *Oct4* gene expression. Quantitative RT-PCR showed that hypoxia (1% O₂) significantly increased *Oct4* gene expression (n = 3) (*p < 0.01). NX: normoxia, HX: hypoxia. **(b)** Hypoxia increases Oct4 protein expression. Oct4 protein expression was measured by western blot analysis. NX: normoxia, HX: hypoxia. **(c)** Expression of Oct4 mRNA in melanoma tissues. Four of five fresh melanoma tissues expressed *Oct4*. **(d)** Immunohistochemical stains of Oct4 in human melanoma tissue. Oct4 showed nuclear staining pattern. Nuclei of some melanoma cells were highlighted. Bar indicates 80 μ m in the left panel and 20 μ m in the right panel.